Solid Freeform Fabrication 2021: Proceedings of the 32nd Annual International
Solid Freeform Fabrication Symposium – An Additive Manufacturing Conference
Reviewed Paper

The Effect of Stress Intensity Factor on Fatigue Life of AM Parts Made from Polymer

H. H. El Fazani[1*], J. D.A. Coil[2], R. R. Shah[3], J. F. Laliberte[4]

**Department of Mechanical and Aerospace Engineering, Carleton University,*

1125 Colonel By Drive, Ottawa, Ontario, K1S-5B6, Canada.

**Corresponding Author (hayatelfazani@cmail.carleton.ca)*

Abstract

The fatigue characteristics of additively manufactured specimens was investigated. A commercial acrylonitrile-butadiene-styrene (ABS) polymer (P430) was selected to manufacture AM fatigue coupons due to its low cost and wide applications. A total of 30 fatigue coupons were built on flat and on edge using a *Stratasys SST 1200es* fused deposition machine. The AM samples were manufactured at different build orientations of 0°, 22.5°, 45°, 67.5°, and 90°. The objective of this experiment is to investigate the influence of stress intensity factor on fatigue life of AM polymer parts. The specimens were tested under low sinusoidal tension-tension fatigue loading. The fatigue crack behaviour was monitored using a travelling microscope method. The stress intensity factor was investigated as the cycles accumulated. The effect of stress intensity factor on fatigue life was examined. The investigation of fatigue crack growth as a function of the number of fatigue cycles was discussed. It was found the fatigue coupons manufactured at 0° build orientation have a better fatigue life compared with the other build orientations. More investigation is required for other AM parameters such as layer thickness, infill density, manufacturing process to help better understand the fatigue performance of AM part made by polymer material. The Scanning Electron Microscope (SEM) technology was used to characterize the fractured surfaces and void distribution of AM fatigue parts. The void percentage was estimated. The results showed that AM fatigue parts built on flat has a higher void percentage compared to the AM parts manufactured on edge.

Keywords

Additive Manufacturing, Fused deposition modelling, Fatigue Crack, Fatigue Coupons, Stress Intensity Factor.

Introduction

Additive manufacturing technology has brought great advantages. However, there is a current need to further study the material behavior of AM parts. The lack of research publication on fatigue analysis for AM polymer parts manufactured by FDM technique was discussed in [1] [2]. For this reason, the fatigue crack propagation behavior for polymers continues to be an active area of study.[3]. Lee *et al.* [4] explored the influence of fatigue on AM part made from ABS material. The study was based on comparing the fatigue life of ABS polymer made by FDM with a bulk precursor material. The results demonstrated that AM polymers have a significantly lower fatigue life. Likewise, it is crucial to consider long term fatigue loading for aircraft applications; ABS 3D printed polymers have very poor fatigue characteristics, which limits their feasibility for application in the aircraft structure, concluded by Schiller [5].

It is necessary to understand the damage propagation mechanics underlying the failure process to ensure the final AM product will not suffer early failure under cyclic loading. Fatigue crack growth testing was conducted to examine both initiation and propagation mechanisms, with a focus on early crack initiation in AM polymer materials. Several fatigue testing methodologies are available and described in the literature [1][4] [6]. The use of a specific method depends on the types of the fluctuating stresses and strains, as well as on the purpose of test. Fatigue tests can be based on reversed stress cycles, repeated stress cycles, or random or irregular stress cycles. These methods are also known as tension – compression fatigue loading, compression – compression fatigue loading, and tension – tension, respectively. Testing for each can be conducted at high cyclic fatigue loading, or low cyclic fatigue loading. The method which involves the opening in tension fatigue mode I was chosen in this experiment. The fatigue test approach that was utilized in this research was based on a tension – tension, low cyclic fatigue loading as shown in Figure 1. The traveling microscope approach was selected for crack detection and monitoring, and crack measurement. The method was chosen because the traveling microscope gives accurate crack measurements both at initiation and during propagation. In this research, the application of damage tolerance and fatigue evaluation and fatigue characteristics of ABS material made by FDM were investigated. This includes investigation of the influence of the stress intensity factor on fatigue life. The fatigue crack growth in AM polymer specimens were monitored and the crack lengths were measured by using a travelling microscope.

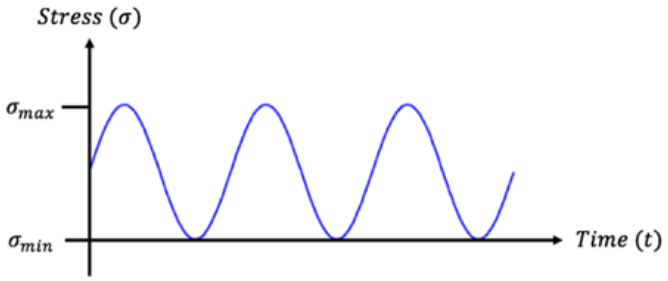

Figure 1: Constant amplitude fatigue.

Methodology

The fatigue life of AM polymer parts was determined by measuring the crack length on AM specimens caused by low cyclic, tension-tension fatigue loading. The fatigue failure of AM parts starts with a crack formation at a point of high stress concentration. This is followed by crack propagation, which ultimately leads to total failure of the component. An optical microscope was used to monitor the crack lengths at initiation and propagation. Table 1 shows the test matrix for fatigue analysis using the travelling microscope. The test matrix was made to investigate the effect of building orientations 0°, 22.5°, 45°, 67.5°, and 90° on the fatigue properties of AM polymers. The parts were manufactured with 0.25 mm layer thickness. The minimum number of proposed fatigue tests for travelling microscope method is 30 tests.

Table 1: Material fatigue test matrix.

AM process and orientations		**Minimum number of acceptable fatigue test**					**Total**
		0°	**22.5°**	**45°**	**67.5°**	**90°**	
Stratasys SST 1200es Layer Thickness 0.25 mm	Flat	4	3	4	3	7	21
	On Edge	3		3		3	9
Total							**30**

Fatigue Test Setup and Procedure

The basic fatigue test consists of a test coupon that is subjected to a cyclic load. The frequency and stress amplitude applied during fatigue testing will cause the polymer to exhibit either thermal softening or cyclic crack growth [7]. The AM fatigue specimen was designed as a large radii dogbone coupon, reducing the possibility of premature specimen failure during cyclic loading while still maintaining a small region of possible crack formation. The MTS machine used for the fatigue testing is shown in Figure 2a. In this research, the specimens were tested under sinusoidal tension-tension fatigue loading at a low frequency of 3 Hz. The maximum applied load was + 0.9 kN and the minimum applied load was zero. The selection of this type of loading condition was based on previous literature [4][8]. Testing the specimen at low frequency eliminates any heating effects due to the strains. As well, using a minimum applied load of zero avoids any bending that might occur from compression. In addition, if a compression load is applied, it becomes very difficult to accurately identify the crack length as the crack will be closed during compression. The undesired compression force may also lead to losing the features of the fracture surface, which are very important to the analysis. A travelling microscope was utilized to observe and measure the cracks with an accuracy of +/- 0.01 mm. A point light source was used to illuminate the specimen surface. The specific type of light was chosen to clearly identify cracks throughout the test. The specimen was gripped axially in the loading direction as shown ion Figure 2b.

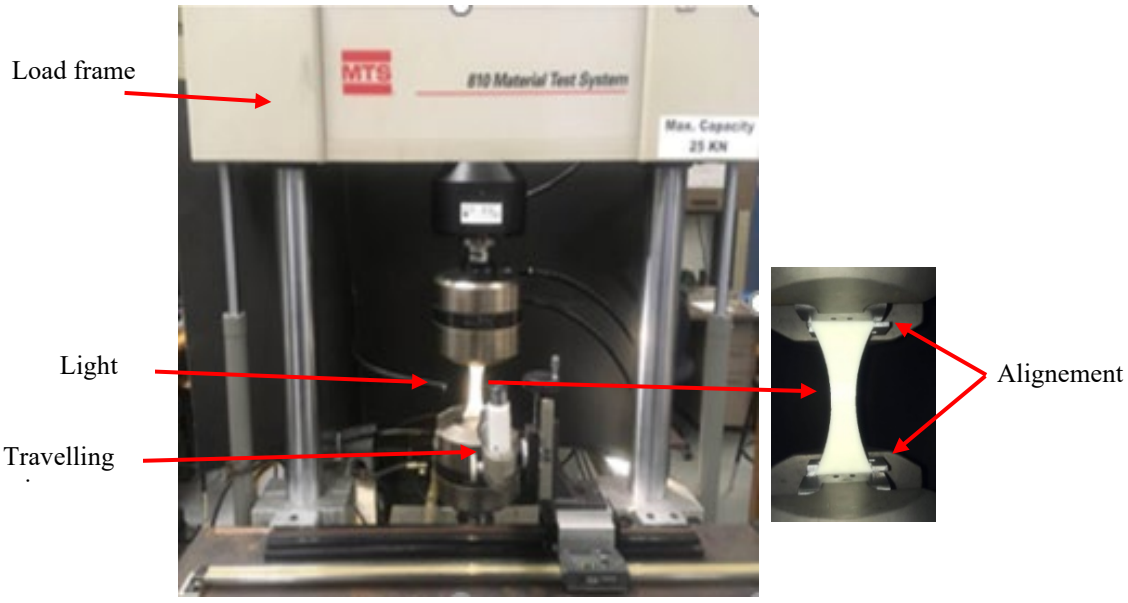

Figure 2: Fatigue test equipment, a. MTS machine, b. Fatigue test specimen aligned fences.

The fatigue test was conducted at room-temperature (approximately 21°C). The specimen surface was observed during loading and unloading. A small crack which started to form and initiate on the gauge length of the tested area was tracked. There are different techniques of crack detection such as the compliance method applied in [9]. The chosen method of crack monitoring was to use travelling microscope, where the crack tip was monitored with a crosshair and with light point assistant as shown in Figure 3. The microscope travels parallel to the crack using a hand cranked vernier mechanism. The travelling microscope has a digital scale readout, allowing a crack measurement within an accuracy of 0.01 mm [10]. The crack propagation was monitored until the crack reached critical dimensions or until a complete specimen failure occurred [11]. The visual microscope approach is considered a reliable method because it gives crack measurements accurate enough to be used to validate other techniques [9]. The first specimen was cycled for 300 cycles. Once this point was reached, the gauge area was carefully observed by using the travelling microscope to identify the cracks. All cracks and their respective lengths were measured and recorded. Images in Figure 3 shows all the cracks formed both on and inside the surface. After crack initiation, continual loading of the stress concentration with additional cycles led to a gradual crack propagation. The crack accelerates over more cycles, which sometimes culminates a sudden failure. These steps were repeated until the specimen failed. The number of cycles at the failure was recorded and all data was saved for analysis. The number of cycles associated with the crack measurements was recorded with the applied loads during the measuring. The speed of an individual crack propagation can be influenced by other cracks surrounding a single crack. It is normal for multiple cracks under cyclic stress fluctuations to grow and come together to form a single long crack. The crack then becomes unstable, resulting in a sudden quick failure which separates the specimen into two parts. SEM analysis was conducted for the fracture surfaces of AM fatigue coupons to investigate the void distribution and to calculate the void volume.

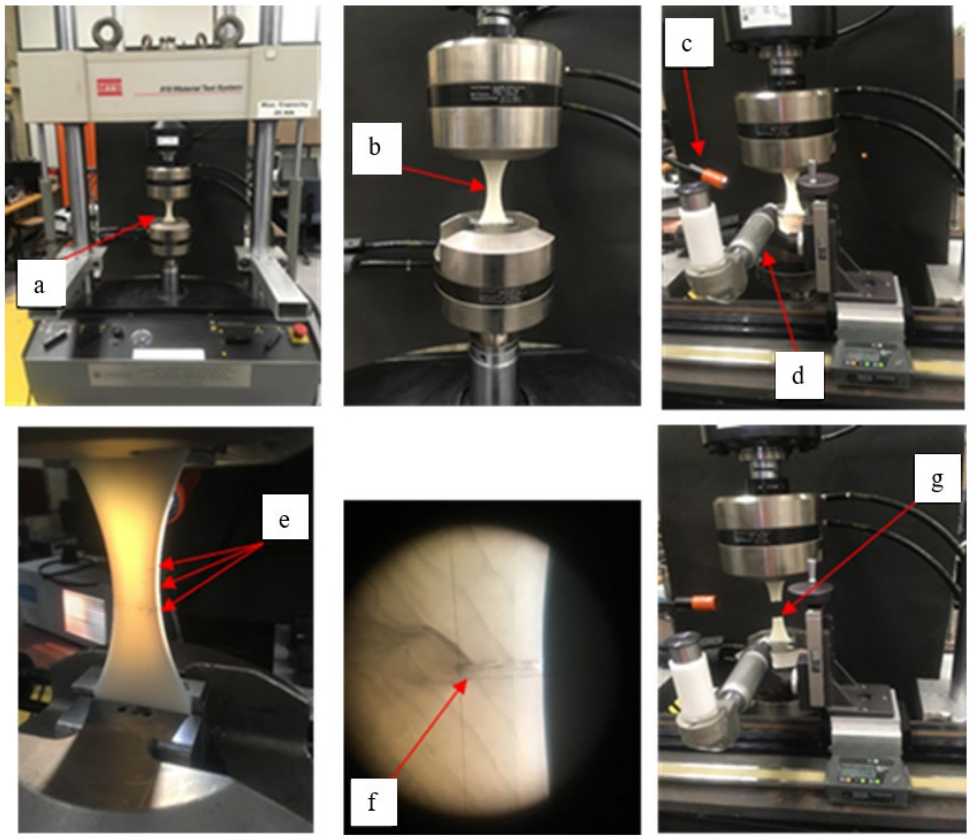

Figure3: Fatigue testing procedure: a. Specimen mounted at 25 kN MTS load frame, b. Under fatigue testing, c. Light source, d. Travel microscope, e. Multiple cracks, f. Single crack length measurement, g. Specimen at failure.

Fatigue Crack Growth Rates as a Function of Stress-Intensity Factor Range (ΔK)

Fatigue crack growth rates was uniquely correlated to stress intensity factor range (ΔK) by Furmanski *et al.* [3]. In literature there are several approaches to determine the cyclic crack growth rate, da/dN , where a is the typical crack length and N is the number of fatigue cycles [9][10] [12] [13]. For example, it was suggested by Bannantine *et al.* [14] and Blattmeier *et al.* [15] that the fatigue crack propagation rates under cyclic loading can be empirically represented by Equation 1, which also known as Paris power law.

$$\frac{da}{dN} = C(\Delta K)^m \tag{1}$$

Where ΔK represents the stress intensity factor range in MPa $m^{1/2}$, C and m are published material constants [11][16] found empirically, showing correlation between the crack growth rate with the amplitude cyclic stress intensity.

By using the crack measurements recorded from the travelling microscope and the number of cycles N displayed in the MTS software, the ranges of stress intensity factor ΔK can be calculated by:

$$\Delta K = K_{max} - K_{min} = f(g)\Delta\sigma\sqrt{\pi a} \quad (2)$$

The maximum load level of 0.9 kN was specified and the minimum load selected to be zero. The stress intensity factor was calculated by using the formula presented in [14]:

$$K_I = f(g)\sigma\sqrt{\pi a} \quad (3)$$

$$f(g) = 1.12 - 0.231\left({}^{a}/_{b}\right) + 10.55\left({}^{a}/_{b}\right)^2 - 21.72\left({}^{a}/_{b}\right)^3 + 30.39\left({}^{a}/_{b}\right)^4 \quad (4)$$

Where a is crack length in mm and b is the specimen width in mm. Figure 4 shows the difference between the two measurements.

A built-in MATLAB algorithm was utilized to solve Equation 4 using the recoded crack lengths with the associated numbers of cycles. The program output provided the crack growth rate values and the change in stress intensity factor.

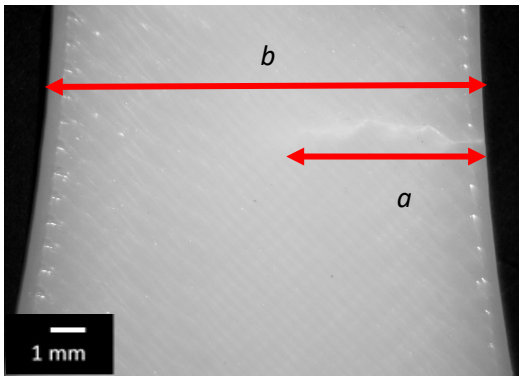

Figure 4: Specimen with crack growth leading up to failure.

Results and discussions

Crack Growth Rates Analysis for Specimens Manufactured with a Flat Layout

The fatigue crack growth rate as a function of stress intensity factor for AM typical part built at 90° orientations is presented in Figure 5. It is important to highlight that Paris law is observably identified in this curve. The specimen was cycled at low cyclic loading and the stress intensity factors were estimated as the cycles were accumulating. It was observed that over time the crack accelerates, and the crack speed increased after reaching a stress intensity value of 0.65 (MPa $m^{1/2}$). To get a better understanding on how the build orientations for AM part may affect the crack growth rates. The results of fatigue crack growth rate as a function of stress intensity factor for a group of specimens manufactured with 0°, 22.5°, 45°, 67.5° and 90° build orientations are illustrated in Figure 6. This graph provides a summary of the crack growth rates (da/dN) for 5 AM specimens. A rapid growth in crack length was observed for AM specimen manufactured with

0° orientation. The crack growth rate reached 0.0015 (m/cycle) at a stress intensity factor value of 0.62 (MPa $m^{1/2}$). It was expected for part built with 90° to have the same behavior but this part exhibits a slower propagation in which that crack growth rates was 0.0006 (m/cycle) at stress intensity factor of nearly 0.77 (MPa $m^{1/2}$). The fatigue crack growth rate for specimens built on 67.5° exhibited the lowest amount in comparison with other specimens. There is clear overlap between the final stage of crack initiation for the part built at 90°. The specimen with a build orientation of 45° demonstrated a gradual increase in crack length.

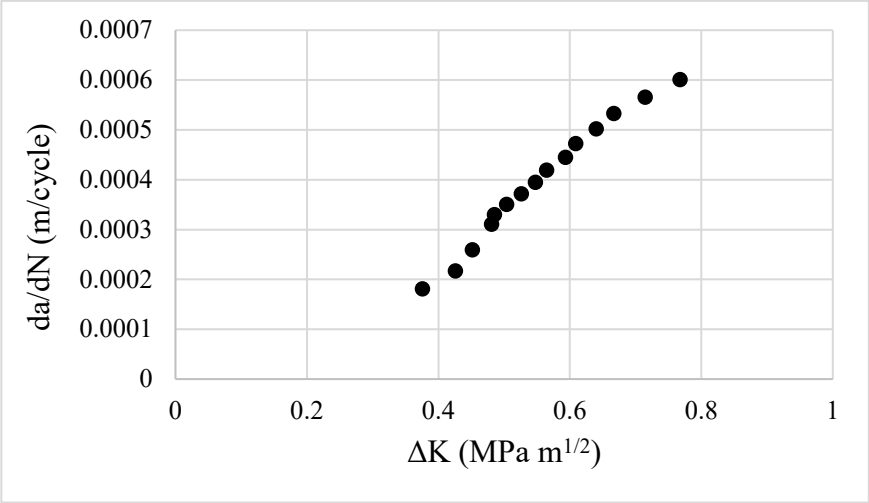

Figure 5: Fatigue crack growth rate for a single crack as a function of stress-intensity factor range (ΔK) for AM specimen manufactured on flat and with 90° build orientations.

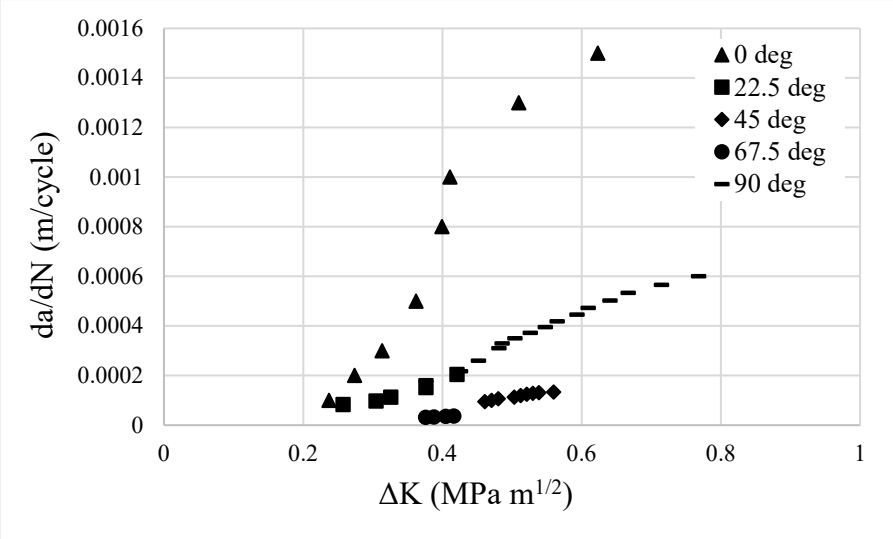

Figure 6: Fatigue crack growth rate for a single crack as a function of stress-intensity factor range (ΔK) for specimens manufactured on flat and with 0°, 22.5°, 45°, 67.5° and 90° build orientations.

The relation between the fatigue crack growth rate (da/dN) and the crack length (a) for a single crack is shown in Figure 7. The presented results are for AM parts made with 0°, 22.5°, 45°, 67.5° and 90° build orientations. It was observed that the AM part manufactured with 0° can survive larger cracks before failure compared to the other orientations.

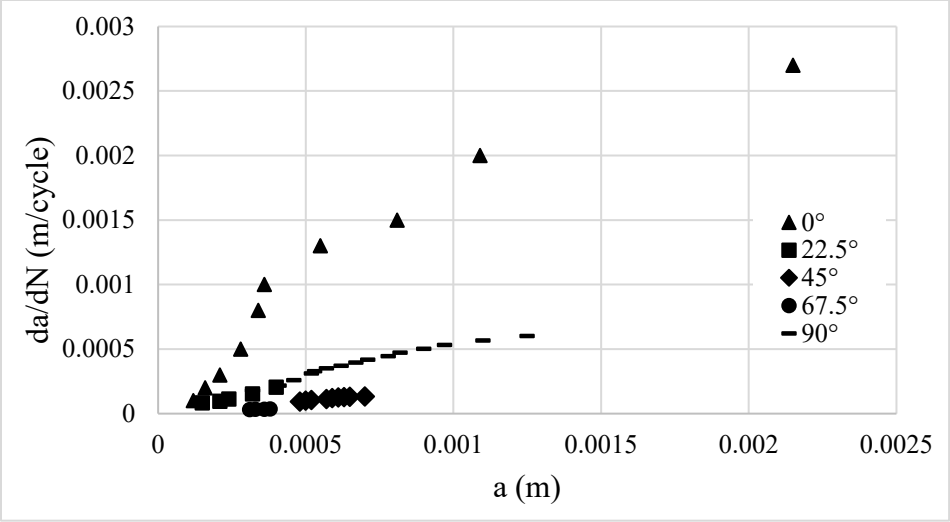

Figure 7: Fatigue crack growth rate for a single crack as a function of crack length for specimens manufactured on flat and with 0°, 22.5°, 45°, 67.5° and 90° build orientations.

Crack Growth Rates Analysis for Specimens Manufactured with on edge

The results of fatigue crack growth rate versus the stress intensity factor for AM part manufactured with 90° build orientations are displayed in Figure 8. The crack growth rate of 3.42 $*10^{-5}$ (m/cycle) was recorded at stress intensity factor of 0.617 (MPa $m^{1/2}$). The crack grew slowly until it reached a rate of $1.1*10^{-4}$ (m/cycle) at an approximate stress intensity factor of 0.94 (MPa $m^{1/2}$). Then the crack speed increased which led to rapid crack propagation. The final stress intensity factor collected is 2.11 (MPa $m^{1/2}$) and the crack growth rate was measured to be $1.83*10^{-4}$ (m/cycle).

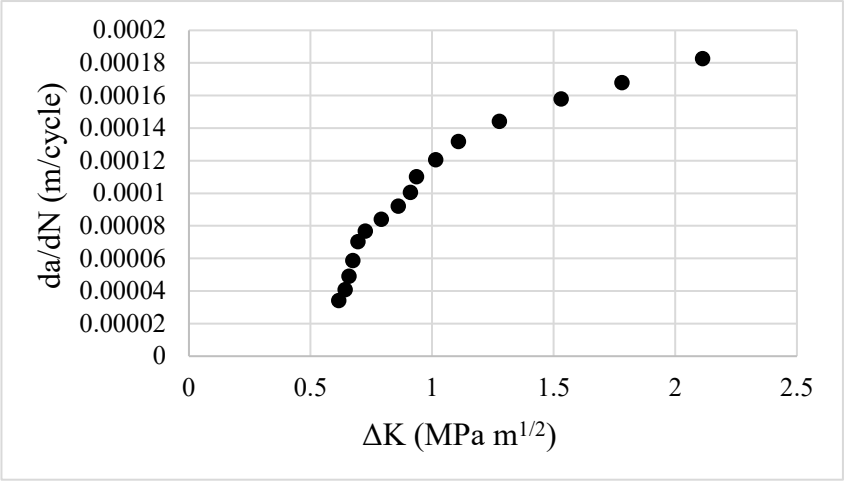

Figure 8: Fatigue crack growth rate for a single crack as a function of stress-intensity factor range (ΔK) for AM specimen manufactured on edge and with 90° build orientations.

Figure 9 shows the results of fatigue crack growth rate versus the stress intensity factor for AM fatigue specimens manufactured on edge and with build angles of 0°,45° and 90°. The AM coupon built with 0° orientations exhibited a higher crack growth in comparison with the 45° and 90° specimens. The highest crack propagation was recorded at 2.13 (MPa $m^{1/2}$) with a value of da/dN of $3*10^{-4}$ (m/cycle). It was also observed that there is an overlap between the AM samples printed at 45° and 90° build angles. This overlap was found within a range of stress intensity factors from 0.75 to 2.11 (MPa $m^{1/2}$). Since the crack growth rate da/dN for AM fatigue coupon built on 45° was found to be as low as 0.001 at 3.5 (MPa $m^{1/2}$). Therefore, it can be argued that the AM part oriented at 45° has a better fatigue life compared to the coupons oriented at 0° and 90° build orientation.

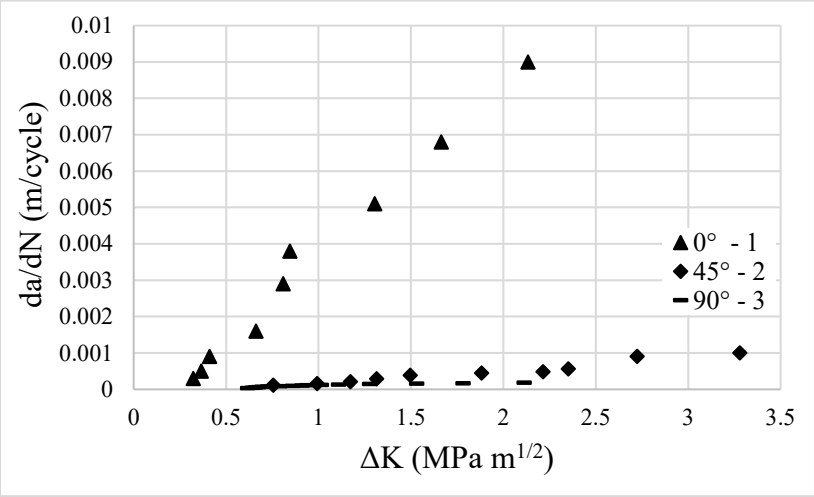

Figure 9: Fatigue crack growth rate for a single crack as a function of stress-intensity factor range (ΔK) for specimens manufactured on edge and with 0°, 45° and 90° build orientations.

Scanning Electron Microscope (SEM) Results

The SEM examination of the fractured surface of AM polymer parts built on flat at 45° build orientations is shown in Figure 10. The surface labeled 1 was close to the building bed and it was built first, surface 2 was built at the end. It is contended that the indicated fracture path followed the weakest portions of the sample. The voids and the cavities formation and interconnection over cyclic loading increased the overall crack length and led to sudden failure. Figure 11 displays the SEM analysis for AM part made on edge side at 90° build orientation using *Stratasys SST 1200es.* The surface labeled 1 was closest to the heated building bed and was deposited first, surface 2 was deposited at the end. The microscopy results show that the filaments in the middle of the cross-section area had better fusion which led to fewer airgaps. It is likely that the specimens experienced a brittle fracture. The fatigue crack features on the surfaces were also highlighted. A voids distribution

AM parts manufactured on flat found to have a higher void percentage of 7.29% compared to the fatigue coupons built on edge with voids percentage 2.26%. This finding support the fatigue crack growth results discussed in the previous section. In other words, the fatigue crack growth

rate was higher for the parts manufactured on flat versus on edge which indicates that the void formation has a critical impact on the fatigue life.

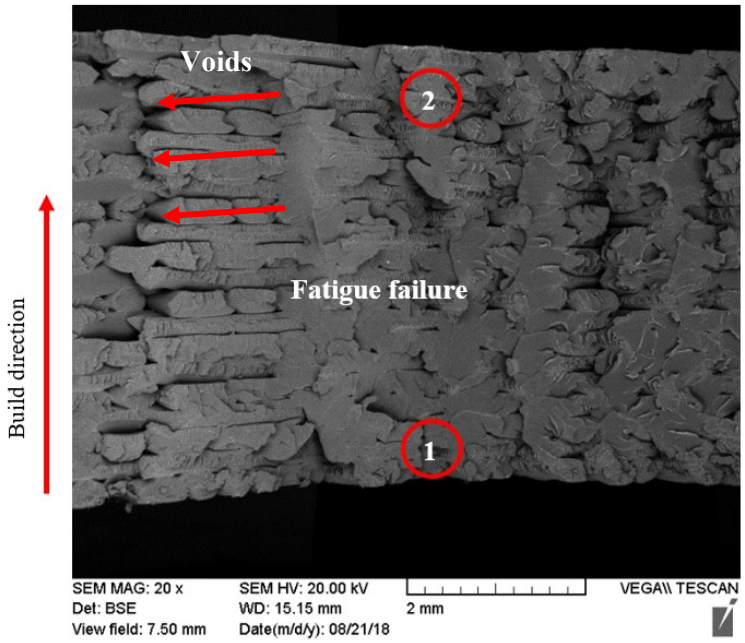

Figure 10: SEM image for the fractured surface of AM fatigue coupon made on the flat side at 45° build orientations using *Stratasys SST 1200es*.

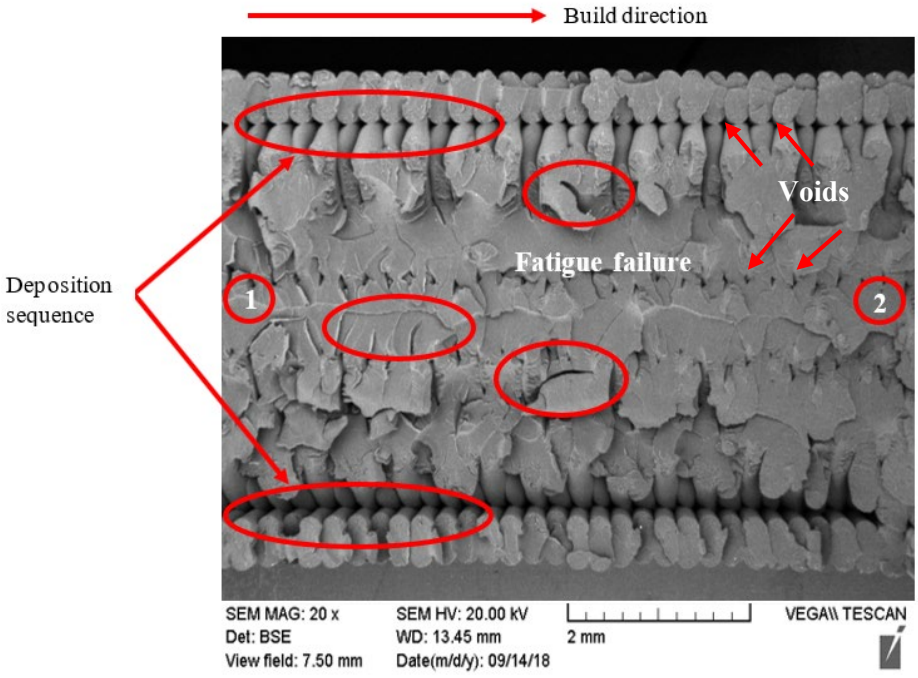

Figure 11: SEM microscopy for the fractured surface of AM fatigue coupon manufactured on edge at 90° build orientation using *Stratasys SST 1200es.*

Conclusion

Fatigue crack investigation was conducted for AM parts made from ABS polymer material. The influence of the stress intensity factor on the fatigue life of AM fatigue coupons was examined. The fatigue crack measurements results for AM polymer specimens showed that the building orientation and the existence of voids within the specimens played a significant role in the fatigue properties. The coupons built at 0° orientation can accumulate more damage and thus have a longer fatigue life as compared to the other four orientations 22.5°, 45°, 67.5° and 90°. SEM analysis was performed for the fractured surface of AM polymer parts. The voids percentage of AM fatigue parts were calculated. The AM parts built of flat found to have a higher voids percentage compared to the AM parts manufactured on edge.

In future work, it is recommended that expand the optical analysis to include Micro Computed Tomography (Micro-CT). Deep investigation is required for the internal structure of AM fatigue parts manufactured at 0° build orientation. This will provide a better understanding the reasons for accumulating longer crack for this specific samples.

Acknowledgements

The authors would like to acknowledge the technical support and training provided by the supervisor of the Mechanical and Aerospace Engineering Laboratories at Carleton University Mr. Steve Truttmann and the assistance in parts fabrication provided by senior laboratory technologist Mr. Stephan Biljan. Also, the current research was made possible by the financial support from the Natural Sciences and Engineering Research Council of Canada (NSERC).

References

[1] S. Ziemian, M. Okwara, and C. W. Ziemian, "Tensile and fatigue behavior of layered acrylonitrile butadiene styrene," *Rapid Prototyp. J.*, vol. 21, no. 3, pp. 270–278, 2015.

[2] C. W. Ziemian, R. D. Ziemian, and K. V. Haile, "Characterization of stiffness degradation caused by fatigue damage of additive manufactured parts," *Mater. Des.*, vol. 109, pp. 209–218, 2016.

[3] J. Furmanski and L. A. Pruitt, "Static mode fatigue crack propagation and generalized stress intensity correlation for fatigue–brittle polymers," *Int. J. Fract.*, vol. 210, no. 1–2, pp. 213–221, 2018.

[4] J. Lee and A. Huang, "Fatigue analysis of FDM materials," *Rapid Prototyp. J.*, vol. 19, no. 4, pp. 291–299, 2013.

[5] G. J. Schiller, "Additive manufacturing for Aerospace," *IEEE Aerosp. Conf. Proc.*, 2015.

[6] N. S. F. Jap, G. M. Pearce, A. K. Hellier, N. Russell, W. C. Parr, and W. R. Walsh, "The effect of raster orientation on the static and fatigue properties of filament deposited ABS polymer," *Int. J. Fatigue*, vol. 124, pp. 328–337, 2019.

[7] J. C. Radon, “Fatigue crack growth in polymers,” *Int. J. Fract.*, vol. 16, no. 6, pp. 533–552, 1980.

[8] M. S. and S. Z. Constance Ziemian, “Anisotropic Mechanical Properties of ABS Parts Fabricated by Fused Deposition Modelling,” in *Intech open*, vol. 2, 2018, p. 64.

[9] Q. Z. Fang, T. J. Wang, and H. M. Li, “‘Tail’ phenomenon and fatigue crack propagation of PC/ABS alloy,” *Polym. Degrad. Stab.*, vol. 93, no. 1, pp. 281–290, 2008.

[10] E. E. Saenz, L. A. Carlsson, G. C. Salivar, and A. M. Karlsson, “Fatigue crack propagation in polyvinylchloride and polyethersulfone polymer foams,” *J. Sandw. Struct. Mater.*, vol. 16, no. 1, pp. 42–65, 2014.

[11] J. M. Barsom, *Fatigue-Crack Propagation in Steels of Various Yield Strengths*, vol. B73, no. 4. 1971.

[12] X. R. Wu, D. H. Tong, X. C. Zhao, and W. Xu, “Review and evaluation of weight functions and stress intensity factors for edge-cracked finite-width plate,” *Eng. Fract. Mech.*, vol. 195, pp. 200–221, 2018.

[13] J. -F Hwang, J. A. Manson, R. W. Hertzberg, G. A. Miller, and L. H. Sperling, “Fatigue crack propagation of rubber-toughened epoxies,” *Polym. Eng. Sci.*, vol. 29, no. 20, pp. 1477–1487, 1989.

[14] J. J. Bannantine, Julie A; Handrock, James L; Comer, *Fundamentals of metal fatigue analysis*. Prentice Hall, 1990.

[15] M. Blattmeier, G. Witt, J. Wortberg, J. Eggert, and J. Toepker, “Influence of surface characteristics on fatigue behaviour of laser sintered plastics,” *Rapid Prototyp. J.*, vol. 18, no. 2, pp. 161–171, 2012.

[16] S. T. Rolfe, “Fracture and Fatigue Control in Structures,” *Engineering*, pp. 1–15, 1977.

[17] K. S. R. Chandran, “Mechanical fatigue of polymers: A new approach to characterize the S-N behavior on the basis of macroscopic crack growth mechanism,” *Polymer (Guildf).*, vol. 91, pp. 222–238, 2016.

[18] T. D. McLouth, J. V. Severino, P. M. Adams, D. N. Patel, and R. J. Zaldivar, “The impact of print orientation and raster pattern on fracture toughness in additively manufactured ABS,” *Addit. Manuf.*, vol. 18, pp. 103–109, 2017.